Damage Detection in Transparent Materials Using Non-Contact Laser Excitation by Nano-Second Laser Ablation and High-Speed Polarization-imaging Camera

N. Hosoya, R. Umino, I. Kajiwara, S. Maeda, T. Onuma & A. Mihara

Experimental Mechanics
An International Journal

ISSN 0014-4851

Exp Mech
DOI 10.1007/s11340-015-0089-y

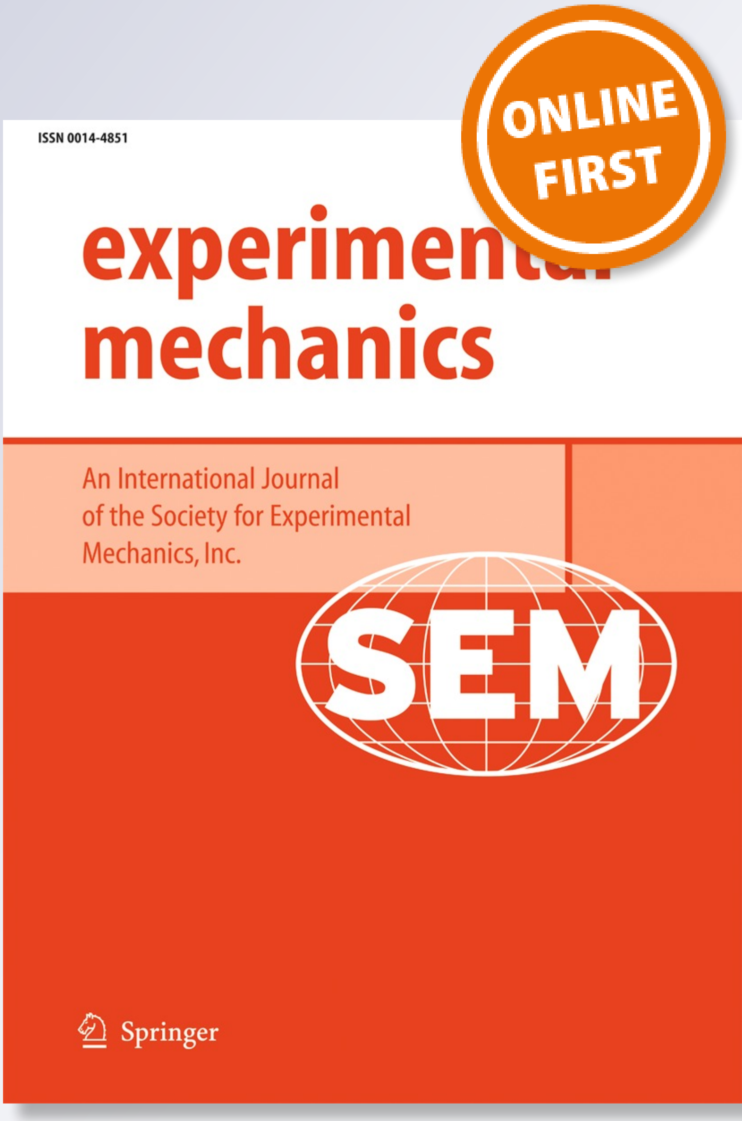

Springer

Experimental Mechanics
DOI 10.1007/s11340-015-0089-y

BRIEF TECHNICAL NOTE

Damage Detection in Transparent Materials Using Non-Contact Laser Excitation by Nano-Second Laser Ablation and High-Speed Polarization-imaging Camera

N. Hosoya[1] · R. Umino[2] · I. Kajiwara[3] · S. Maeda[1] · T. Onuma[4] · A. Mihara[4]

Received: 9 December 2014 / Accepted: 25 August 2015

Abstract Although transparent materials with birefringent properties (e.g., solar panels and separator films for secondary cells) are common, damage detection during the manufacturing process is crucial to economically realize high-quality materials. Herein a method using a pulsed-laser and a high-speed polarization-imaging camera is proposed to rapidly detect damage, including scratches and dents, in transparent materials. Specifically, as stress waves, which are generated by a non-contact impulse excitation from laser ablation, propagate through a material, the stress concentrations induced around damage are measured as the two-dimensional birefringent phase differences using a high-speed polarization-imaging camera with a microsecond-order temporal resolution. When stress is dominant, the distribution of the measured birefringent phase difference can be considered the relative distribution of stress. Using acrylic plates as a representative transparent material with several hundred micrometers of damage (e.g., a dent or a scratch), we demonstrate that the proposed method detects damage in a very short timeframe of several microseconds.

Keywords Damage detection · Non-contact laser excitation · Nanosecond laser ablation · Transparent material · Two-dimensional birefringent distribution · High-speed polarization-imaging camera

Introduction

In recent years, the demand for transparent optical materials with birefringent properties (herein "transparent materials") has greatly increased. For example, transparent materials are used in solar panels and separator films for secondary cells, including lithium-ion batteries in the energy field, as well as in phase difference films for liquid crystal displays such as smartphones and tablet devices in the information technology field. To economically fabricate high-quality optical materials, detecting damage (e.g., scratches, dents, cracks, and through-holes) during the manufacturing process is critical. Although many damage detection methods have been developed, they cannot detect damage smaller than about several micrometers.

✉ N. Hosoya
hosoya@sic.shibaura-it.ac.jp

R. Umino
md14009@shibaura-it.ac.jp

I. Kajiwara
ikajiwara@eng.hokudai.ac.jp

S. Maeda
maeshin@sic.shibaura-it.ac.jp

T. Onuma
oonuma@photron.co.jp

A. Mihara
mihara@photron.co.jp

1 Department of Engineering Science and Mechanics, Shibaura Institute of Technology, 3-7-5 Toyosu, Koto-ku, Tokyo 135-8548, Japan

2 Division of Mechanical Engineering, Shibaura Institute of Technology, 3-7-5 Toyosu, Koto-ku, Tokyo 135-8548, Japan

3 Division of Human Mechanical Systems and Design, Hokkaido University, N13, W8, Kita-ku, Sapporo 060-8628, Japan

4 Imaging Division, Photron Limited, 21F, Jinbocho Mitsui Bldg, 1-105 Kanda Jinbocho, Chiyoda-ku, Tokyo 101-0051, Japan

Published online: 03 September 2015

Many damage detection technologies use vibration and acoustic testing. Traditional methods range from those based on hammer tapping to those that use a combination of lead zirconate titanate (PZT), an acoustic emission (AE) sensor, a strain gauge, an accelerometer, a laser Doppler vibrometer (LDV), an optical coherence tomography (OCT), and a laser ultrasonic [1–26]. These methods capture the changes in an object's dynamic characteristics (e.g., frequency response function measurements, and wavelet and modal analyses) [5–9], or visualize Lamb waves [10–25]. Unfortunately traditional contact-type input–output measuring devices cannot detect damage in transparent materials during the manufacturing process (e.g., a film fabrication process that includes melting, casting, extending, and rolling).

Although optical output measuring devices (e.g., LDV) can be used to detect damage (e.g., a damage detection method based on a Lamb wave [10, 13, 16, 18–22, 24, 25]), they provide time-consuming point (one-dimensional) measurements, which are not applicable to actual manufacturing processes. On the other hand, stress waves tend to concentrate around damage. This phenomenon can be used to detect damage as waves propagate inside a material.

Laser ablation (LA), which is a process where a high-power laser is focused and irradiated onto a solid, can generate waves. Because the surface temperature of the solid rapidly increases, the surface explosively releases atoms, molecules, ions, etc. [26–36]. LA has been applied to various fields, including the propulsion of flying objects [27], acoustic waves focusing in water [28], generation of multiple stress waves [29], surface modification [30, 31], and sound source generation in acoustic tests [32]. Previously, we proposed a non-contact vibration test to measure the frequency response functions in target structures [33–36].

In this study, stress waves are generated by non-contact impulse excitation using LA (herein after referred to as "LA excitation") [29, 33–36]. Then damage is detected by measuring the stress concentrations as the birefringent phase difference (hereafter referred to as birefringence) using a high-speed polarization-imaging camera [37, 38] with a microsecond-order temporal resolution. Although birefringence depends on a variety of factors (e.g., the structure, orientation, object form, stress, etc.), when stress is predominant, the distribution of the measured birefringence can be considered the relative distribution of stress. Thus, the photographed birefringence realizes a two-dimensional measurement. The proposed method can detect minute damage induced during the manufacturing process. In addition, increasing the lens magnification should allow damage less than about several micrometers to be detected.

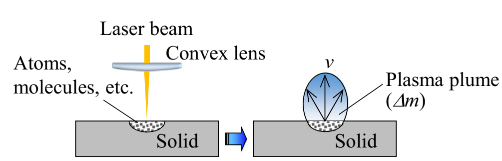

Fig. 1 Principle of the impulse excitation force generated by LA

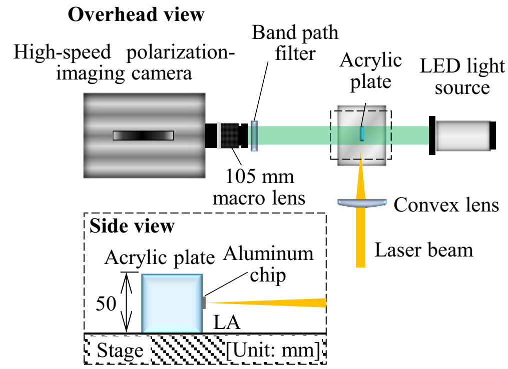

Fig. 2 Experimental system to visualize the two-dimensional birefringence using LA

Materials and Methods

Laser Ablation (LA) [33–36]

Although LA can generate a very small crater on an irradiated surface, the proposed method adopts a pulsed high-power laser to trigger instantaneous LA on an irradiated surface, yielding an ideal impulse excitation input. Figure 1 shows the principle of LA excitation. A solid absorbs the illuminated laser beam, releasing atoms, molecules, and their ions from the solid, which subsequently absorb the laser beam to form a high-temperature, high-density plasma plume composed of

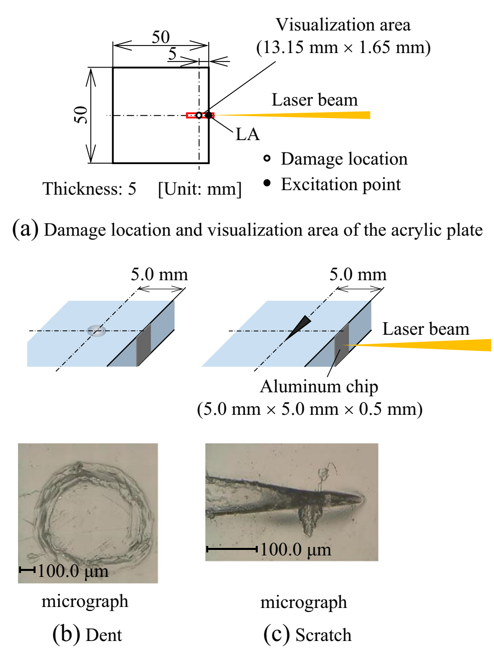

Fig. 3 Test pieces containing damage

Table 1 Configuration of damage

	Damage	Shape	Size [μm]		
Case 1	Dent	Ellipse	Major axis: 845	Minor axis: 574	Depth: 12
Case 2	Scratch	Triangle	Base: 109	Height: 577	Depth: 37

free electrons, ionized atoms, etc. When mass Δm is released at velocity v from a solid, a momentum (Δmv) is generated, which induces stress waves within a transparent material. Because the plasma plume is released normal to from the solid surface's tangent plane, the impulse direction is normal to the solid surface. LA is produced when the laser fluence reaches 10^{12}–10^{14} W/m^2 [32–36, 39].

Experimental Setup

This study aims to realize non-contact damage detection by evaluating the propagation of stress waves (the propagation of the birefringence) generated by LA. In this study, damage in acrylic, which is used a representative transparent material, is detected by generating a stress wave using LA excitation. Then the propagation of birefringence is photographed using a high-speed polarization-imaging camera. Figure 2 shows our two-dimensional birefringent distribution measurement system and a test piece. This system consists of an Nd:YAG pulsed-laser (Continuum surelite III-10, wavelength: 1064 nm, beam diameter: 9.5 mm, pulse duration: 5 ns, maximum output: 1 J, and divergence: 0.5 mrad) and a high-speed polarization-imaging camera to measure birefringence (Photron Limited CRYSTA PI-1P) (Fig. 2). This device is set on an optical surface plate.

The test piece is an acrylic plate (size: 50×50×5 mm) (Fig. 2). Irradiating the plate with a laser beam (pulse energy: 900 mJ) induces LA on the side surface, which generates a stress wave inside the piece. The beam is concentrated using a convex lens (focal length: 100 mm). In addition, an aluminum plate (size: 5×5×0.5 mm) is attached on the irradiated part of the test piece with adhesive as an ablation material. However, an ablation material is unnecessary in real conditions because LA can be generated against a high-polymer material, metal, etc.

Photographs are acquired with a high-speed polarization-imaging camera (photographing speed: 930,000 fps, exposure time: 0.8 μs, and pixel count: 128×16 (in 13.15×1.64 mm)). Figure 3(a) shows the photographed area. The light source is a green LED (operating wavelength: 480–540 nm, bandwidth of the band path filter: 520±10 nm, and power of the incident light: 75 W/m^2). Laser irradiation and the initial opening of the camera's shutter are synchronized. After 100 ns of a TTL signal from the pulsed-laser system, a laser beam is irradiated. Using the camera's trigger mode "Random Reset", the first image is photographed by the camera after 250 ns of the laser beam irradiation (350 ns of the TTL signal from the pulsed-laser system).

Damage

Figure 3 and Table 1 show the two different types of damage investigated: a dent (Fig. 3(b) and a scratch (Fig. 3(c)). Both occur around the surface. This system should be applicable to damaged areas less than 2 μm by increasing the lens magnification of the high-speed polarization-imaging camera because such a camera with a 20-fold lens can visualize the two-dimensional birefringence in a measurement area less than 2 μm. However, to verify the fundamental detection performance of this system, the induced damage in the experiments is about 100 μm and 5 mm away from the excitation point (Fig. 3(a)).

Results and Discussion

Figure 4 shows the detection performance of the system for pieces with (a) no damage, (b) a dent, and (c) a scratch. Images were acquired before and after laser irradiation (0.250 μs after and above). A larger number indicates a larger measured birefringence [37, 38]. Additionally, the stress waves generated

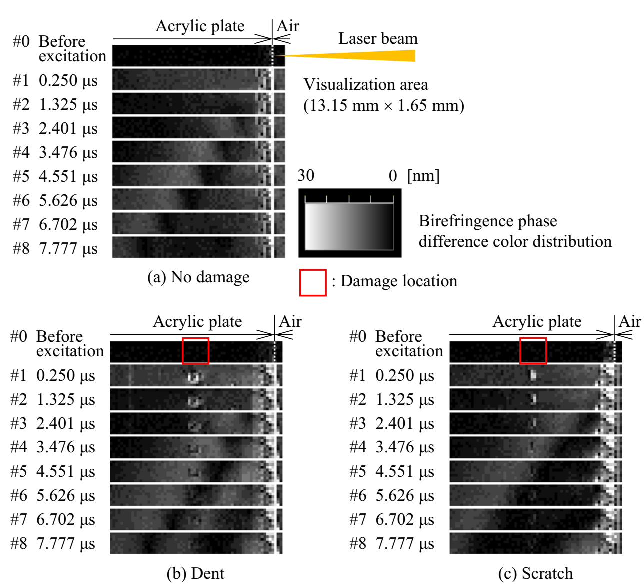

Fig. 4 Time-resolved birefringent images of LA excitation at 900 mJ on an acrylic plate recorded with seven different delay times

by LA excitation are photographed; the waves propagate in a circular-arc-like shape centered at the excitation point, which is similar to previous findings [29].

The birefringence spreads throughout the visualized areas (#1 (0.250 μs) of Fig. 4(a)), whereas the area with a large measured birefringence gradually moves to the left. The propagation velocities of the longitudinal wave and transverse wave are 2690–2756 and 1340–1401 m/s, respectively [40]. The velocity of the transverse wave agrees with the calculated velocities based on Fig. 4 (approximately 1500 m/s), indicating that the visualized stress waves detected by measuring the birefringence with this system include the transverse wave. Because the longitudinal wave velocity is 2690–2756 m/s, it must be visualized in #1 and #2 of Fig. 4. Due to the insufficient time-space resolution to visualize the longitudinal wave, calculating the longitudinal wave velocity by image analysis based on Fig. 4 is difficult.

The damaged areas in Fig. 4(b) and (c) have relatively large measured birefringences at #1 (0.250 μs) and #4 (3.476 μs) because the stress waves that propagate within the test pieces (longitudinal and transverse waves) are concentrated around the damage and are measured as birefringence. Longitudinal waves should be able to detect more minute damage because a larger birefringence is generated as longitudinal waves propagate. In addition, measurements prior to LA excitation (#0 in Fig. 4(b) and (c)) indicate that the birefringence measured around the damage is similar to the birefringence measured in other areas, suggesting that the measured birefringence plays an important role in damage detection. These results demonstrate that this system can detect damage in transparent materials in a very short timeframe of several microseconds.

Conclusion

We constructed a non-contact excitation system that detects damage in transparent materials during the manufacturing process. Our rapid detection method consists of two steps: stress wave generation and detection of birefringence. LA, which is induced using high-power Nd:YAG pulsed-laser irradiation toward the transparent material, generates stress waves. Then damage is detected as the birefringence using a high-speed polarization-imaging camera to measure the stress concentration of the propagating wave. We compared the longitudinal and transverse waves to identify the most suitable wave for damage detection.

Then we demonstrated the feasibility of this system to detect damage using acrylic plates with damage (e.g., a dent or a scratch). Our system can detect damage in a very short timeframe of several microseconds. More experimental configurations such as the distance to the edge of damage, severity of damage, etc. will be examined in the near future.

Acknowledgments This study was supported by Grants-in-Aid for Challenging Exploratory Research (26630080) and (26630102) from the Japan Society for the Promotion of Science.

References

1. Morikawa SRK, Gama AL, Braga AMB, Correia RR (2005) Monitoring surface breaking defects with piezoelectric active systems. Exp Mech 45:89–95. doi:10.1177/0014485105051303
2. Park S, Ahmad S, Yun CB, Roh Y (2006) Multiple crack detection of concrete structures using impedance-based structural health monitoring techniques. Exp Mech 46:609–618. doi:10.1007/s11340-006-8734-0
3. Gama AL, Morikawa SRK (2008) Monitoring fatigue crack growth in compact tension specimens using piezoelectric sensors. Exp Mech 48:247–252. doi:10.1007/s11340-007-9086-0
4. Liu P, Groves RM, Benedictus R (2014) 3D monitoring of delamination growth in a wind turbine blade composite using optical coherence tomography. NDT Int 64:52–58. doi:10.1016/j.ndteint.2014.03.003
5. Garescì F, Catalano L, Petrone F (2006) Experimental results of a damage detection methodology using variations in modal parameters. Exp Mech 46:441–451. doi:10.1007/s11340-006-8151-4
6. Pandurangan P, Buckner GD (2006) Vibration analysis for damage detection in metal-to-metal adhesive joints. Exp Mech 46:601–607. doi:10.1007/s11340-006-8736-y
7. Montalvão D, Ribeiro AMR, Duarte-Silva JAB (2011) Experimental assessment of a modal-based multi-parameter method for locating damage in composite laminates. Exp Mech 51:1473–1488. doi:10.1007/s11340-011-9472-5
8. Arora V, Wijnant YH, de Boer A (2014) Acoustic-based damage detection method. Appl Acoust 80:23–27. doi:10.1016/j.apacoust.2014.01.003
9. Huda F, Kajiwara I, Hosoya N (2014) Damage detection in membrane structures using non-contact laser excitation and wavelet transformation. J Sound Vib 333:3609–3624. doi:10.1016/j.jsv.2014.04.008
10. Su Z, Lin Ye L, Lu Y (2006) Guided Lamb waves for identification of damage in composite structures: a review. J Sound Vib 295:753–780. doi:10.1016/j.jsv.2006.01.020
11. Cernadas D, Trillo C, Doval ÁF, López Ó, López C, Dorrío BV, Fernández JL, Pérez-Amor M (2006) Non-destructive testing of plates based on the visualisation of Lamb waves by double-pulsed TV holography. Mech Syst Signal Process 20:1338–1349. doi:10.1016/j.ymssp.2005.11.014
12. Kudela P, Ostachowicz W, Żak A (2008) Damage detection in composite plates with embedded PZT transducers. Mech Syst Signal Process 22:1327–1335. doi:10.1016/j.ymssp.2007.07.008
13. Lammering R (2010) Observation of piezoelectrically induced lamb wave propagation in thin plates by use of speckle interferometry. Exp Mech 50:377–387. doi:10.1007/s11340-009-9233-x
14. Lee JR, Yoon CY (2010) Development of an optical system for simultaneous ultrasonic wave propagation imaging at multi-points. Exp Mech 50:1041–1049. doi:10.1007/s11340-009-9293-y
15. Kim MK, Kim EJ, An YK, Park HW, Sohn H (2011) Reference-free impedance-based crack detection in plates. J Sound Vib 330:5949–5962. doi:10.1016/j.jsv.2011.07.025
16. Pohl J, Willberg C, Gabbert U, Mook G (2012) Experimental and theoretical analysis of Lamb wave generation by piezoceramic actuators for structural health monitoring. Exp Mech 52:429–438. doi:10.1007/s11340-011-9503-2

17. Liu XL, Jiang ZW, Ji L (2013) Investigation on the design of piezoelectric actuator/sensor for damage detection in beam with lamb waves. Exp Mech 53:485–492. doi:10.1007/s11340-012-9646-9
18. Valle C, Littles JW Jr (2002) Flaw localization using the reassigned spectrogram on laser-generated and detected Lamb modes. Ultrasonics 39:535–542. doi:10.1016/S0041-624X(02)00249-4
19. Silva MZ, Gouyon R, Lepoutre F (2003) Hidden corrosion detection in aircraft aluminum structures using laser ultrasonics and wavelet transform signal analysis. Ultrasonics 41:301–305. doi:10.1016/S0041-624X(02)00455-9
20. Clorennec D, Prada C, Royer D, Murray TW (2006) Laser impulse generation and interferometer detection of zero group velocity Lamb mode resonance. Appl Phys Lett 89:024101. doi:10.1063/1.2220010
21. Prada C, Clorennec D, Murray TW, Royer D (2009) Influence of the anisotropy on zero-group velocity Lamb modes. J Acoust Soc Am 126:620–625. doi:10.1121/1.3167277
22. Lee JR, Shin HJ, Chia CC, Dhital D, Yoon DJ, Huh YH (2011) Long distance laser ultrasonic propagation imaging system for damage visualization. Opt Laser Eng 49:1361–1371. doi:10.1016/j.optlaseng.2011.07.011
23. Dhital D, Lee JR (2012) A fully non-contact ultrasonic propagation imaging system for closed surface crack evaluation. Exp Mech 52:1111–1122. doi:10.1007/s11340-011-9567-z
24. Cès M, Royer D, Prada C (2012) Characterization of mechanical properties of a hollow cylinder with zero group velocity Lamb modes. J Acoust Soc Am 132:180–185. doi:10.1121/1.4726033
25. Balvantín A, Baltazar A, Rodriguez P (2014) Characterization of laser generated Lamb wave modes after interaction with a thickness reduction discontinuity using ray tracing theory. Exp Mech 54:743–752. doi:10.1007/s11340-013-9846-y
26. The Institute of Electrical Engineers of Japan (1999) Laser ablation and applications. Corona Publishing Co., LTD, Tokyo
27. Yabe T, Phipps C, Yamaguchi M, Nakagawa R, Aoki K, Mine H, Ogata Y, Baasandash C, Nakagawa M, Fujiwara E, Yoshida K, Nishiguchi A, Kajiwara I (2002) Microairplane propelled by laser driven exotic target. Appl Phys Lett 80:4318. doi:10.1063/1.1485313
28. Ko SH, Ryu SG, Misra N, Pan H, Grigoropoulos CP, Kladias N, Panides E, Domoto GA (2007) Laser induced short plane acoustic wave focusing in water. Appl Phys Lett 91:051128. doi:10.1063/1.2768192
29. Hu H, Wang X, Zhai H, Zhang N, Wang P (2010) Generation of multiple stress waves in silica glass in high fluence femtosecond laser ablation. Appl Phys Lett 97:061117. doi:10.1063/1.3479919
30. Alfano M, Lubineau G, Furgiuele F, Paulino GH (2011) On the enhancement of bond toughness for Al/epoxy T-peel joints with laser surface treated surfaces. Int J Fract 171:139–150. doi:10.1007/s10704-011-9636-4
31. Alfano M, Lubineau G, Furgiuele F, Paulino GH (2012) Study on the role of laser surface irradiation on damage and decohesion of Al/epoxy bonded joints. Int J Adhes Adhes 39:33–41. doi:10.1016/j.ijadhadh.2012.03.002
32. Hosoya N, Kajiwara I, Inoue T, Umenai K (2014) Non-contact acoustic tests based on nanosecond laser ablation: generation of a pulse sound source with a small amplitude. J Sound Vib 333:4254–4264. doi:10.1016/j.jsv.2014.04.050
33. Kajiwara I, Hosoya N (2011) Vibration testing based on impulse response excited by laser ablation. J Sound Vib 330:5045–5057. doi:10.1016/j.jsv.2010.09.036
34. Hosoya N, Kajiwara I, Hosokawa T (2012) Vibration testing based on impulse response excited by pulsed-laser ablation: Measurement of frequency response function with detection-free input. J Sound Vib 331:1355–1365. doi:10.1016/j.jsv.2011.10.034
35. Huda F, Kajiwara I, Hosoya N, Kawamura S (2013) Bolt loosening analysis and diagnosis by non-contact laser excitation vibration tests. Mech Syst Signal Process 40:589–604. doi:10.1016/j.ymssp.2013.05.023
36. Hosoya N, Kajiwara I, Umenai K (2015) Dynamic characterizations of underwater structures using non-contact vibration test based on nanosecond laser ablation in water: investigation of cavitation bubbles by visualizing shockwaves using the Schlieren method. J Vib Control. doi:10.1177/1077546314564693
37. Onuma T, Otani Y (2012) A dynamic measurement system for two-dimensional birefringence distribution with sub-millisecond time resolution. J Jpn Soc Precis Eng 78:1082–1086
38. Onuma T, Otani Y (2014) A development of two-dimensional birefringence distribution measurement system with a sampling rate of 1.3 MHz. Opt Commun 315:69–73. doi:10.1016/j.optcom.2013.10.086
39. Torrisi L, Borrielli A, Margarone D (2007) Study on the ablation threshold induced by pulse lasers at different wavelengths. Nucl Instrum Meth B 255:373–379. doi:10.1016/j.nimb.2006.12.144
40. Hartmann B, Jarzynski J (1974) Immersion apparatus for ultrasonic measurements in polymers. J Acoust Soc Am 56:1469–1477. doi:10.1121/1.1903466